Stark-profile calculations for resonance lines of heliumlike argon in dense plasmas

Hans R. Griem and Milan Blaha
Laboratory for Plasma Research, University of Maryland, College Park, Maryland 20742

Paul C. Kepple
Plasma Physics Division, Naval Research Laboratory, Washington, D.C. 20375
(Received 22 March 1989)

The photon energy distributions of the first three resonance lines of heliumlike argon broadened by the local fields of both ions and electrons are calculated for dense H, D, or T plasmas containing small amounts of argon. The electron collisions are treated by an impact theory allowing for both widths and shifts in the distorted-wave approximation to all significant orders of the multipole expansion for the electron-radiator interaction. Ion effects are treated in the quasistatic approximation for dipole interactions between ions and radiators. These interactions between states of a given principal quantum number are calculated in the intermediate-coupling representation, using ion-field-strength distribution functions calculated by Boercker with the method of Iglesias *et al* [Phys. Rev. A **28**, 1667 (1983)]. The profiles obtained were corrected for thermal Doppler broadening and also for ion-dynamical effects according to Stamm *et al.* [Phys. Rev. A **34**, 4144 (1986)].

I. INTRODUCTION

Stark-broadened spectral lines emitted or absorbed by dense high-temperature plasmas are of interest in three contexts: determination of charged-particle densities, radiative energy transport, and, possibly, in measurements of electric fields. Lines from one-electron ions have so far been given the most theoretical attention, both because of the perceived simplicity of their profiles and also because hydrogen and one-electron ion lines are especially sensitive to Stark effects. In measured spectra, lines from two-electron ions are usually more prominent, because they have significant intensities over a broader range of plasma conditions. They are accordingly very useful in density measurements of laser-driven implosions of DT pellet plasmas seeded with argon.[1] The calculated Ar XVII profiles used in this early work to fit the observed profiles had been obtained by scaling electron collisional broadening calculated[2] for one-electron ions and by replacing the usual linear Stark effect treatment of the quasistatic effects of ion-ion interactions[3] by Stark effects valid for any field strength. The latter treatment also allowed inclusion of the effects of intermediate coupling.[4]

We have performed distorted-wave calculations for the electron-ion scattering on the various initial states of Ar XVII involved, to all significant orders in the electric multipole interaction. Moreover, recently progress has been made on three important aspects of the line-broadening problem for one-electron ions, namely on the dynamical effects of ion-ion interactions,[5] and in regard to calculating shifts from electron-ion interactions[6,7] and ion-field-strength distribution functions for high-density plasmas.[8] We include such and other line shifts and also estimate ion-dynamical corrections, i.e., profile smoothing relative to profiles obtained with the quasistatic approximation (and using field-strength distribution functions) for the broadening by ions.

In Sec. II of this paper the general theory used is summarized. Section III describes the result of our electron broadening calculations. We then discuss electron-collisional shifts before presenting in Sec. V calculated profiles for optically thin and homogeneous plasmas.

II. GENERAL THEORY

Our starting point is the line-shape expression[3] derived from the generalized impact broadening approximation for the effects caused by electrons, convolved with the quasistatic Stark profile corresponding to the ion-produced plasma microfield:

$$L(\Delta\omega)=-\frac{1}{\pi}\mathrm{Re}\,\mathrm{Tr}\int_0^\infty dF W(F) \times\{D(F)[i\Delta\omega-i\Delta\omega(F)+\phi]^{-1}\}\ . \tag{1}$$

The expression in curly brackets is the generalized impact profile, and $\Delta\omega$ is the frequency separation from the unperturbed line due to a transition from $(1snp)^1P_1$ to the ground state, i.e., $(1s^2)^1S_0$. The quantity $\Delta\omega(E)$ gives the positions of the various nl levels as a function of the electric field strength F relative to the zero-field position of $(1snp)^1P_1$. The distribution of the field strengths[8] is described by the function $W(F)$, Re indicates the real part, and the trace Tr is over the field-dependent states of the radiating ion for which the principal quantum number equals that of the upper state of the line in question. The operator $D(F)$ generates products of dipole matrix elements which describe relative intensities of allowed and (field-induced) forbidden components corresponding to transitions to the ground state. An implicit assumption here is that all contributing upper levels of given principal quantum number are equally populated. The operator ϕ describes the effects of electron collisions. Its matrix elements will be evaluated in Secs. III and IV.

To calculate the quasistatic Stark effects for arbitrary field strengths, although they should not be so large as to cause significant mixing of states with different principal quantum numbers, one has to solve the system of equations

$$\sum_{l,k}\left\{[\omega_l^k(0)-\omega_{\alpha m}^k(F)]\delta_{l'l}^{k'k}+\frac{e}{\hbar}Fz_{l'l}^{k'k}(m)\right\}\langle\alpha_m^{k'}|\,^k lm\rangle=0\ . \tag{2}$$

This system is obtained from the Schrödinger equation for the perturbed ion in a given external field F, using the $^k lm$ basis. The quantum numbers l,m are the usual quantum numbers for the excited electron, while $k=1,3$ designates the dominant multiplicity. In other words, we use, e.g.,

$$|\,^3lm\rangle=a|\,^3D\rangle+b|\,^1D\rangle\ , \tag{3a}$$

$$|\,^1lm\rangle=b|\,^3D\rangle-a|\,^1D\rangle\ , \tag{3b}$$

with the coefficients a and b taken from intermediate-coupling atomic structure calculations.[9] Corresponding multipliers of hydrogenic matrix elements to obtain the matrix elements $\langle\,^{k'}l'm|z|\,^k lm\rangle=z_{l'l}^{k'k}$ are given in Table I, together with relative energies of the zero-field levels.[10]

We neglect direct singlet-triplet mixing of the S and P levels, for which actual values of the squares of the minority admixture coefficients[9,11] are less than 2% for $n\leq 4$, averaged over J values and corresponding to relative intensities of the intercombination lines of less than 2% of the optically thin resonance lines at high densities, where relative upper level populations are statistical. Especially for $2\,^3P$, this may be an underestimate, and a suitable normalized line should then be added with about the same shape as the resonance line but shifted by ~ 16 eV to lower energies. Fine structure is neglected also, which is easily justified, e.g., compared to thermal Doppler broadening, except, perhaps, for $3p\,^3P$ and $4p\,^3P$, where the fine-structure splitting reaches ~ 1 and 0.4 eV, respectively. These levels are involved because field strengths are often high enough for significant Stark mixing of ^1P and ^{3}D levels, which in turn Stark mix with ^3P and ^{3}S. Under these conditions, there are also significant Stark shifts so that the neglected fine-structure splitting is not important numerically.

Since we neglect intercombination lines caused by intermediate coupling, the matrix elements of $D(F)$ can be written as

$$\langle\alpha_m^{k'}|D(F)|\alpha_m^k\rangle=\tfrac{1}{3}\langle\alpha_m^{k'}|\,^1 1m\rangle\langle\alpha_m^k|\,^1 1m\rangle\ , \tag{4}$$

because the dipole matrix elements between the $|\,^1 1m\rangle$ states and the ground state cancel on area normalization of the profiles. The required matrix elements of ϕ are

$$\langle\alpha_m^{k'}|\phi|\alpha_m^k\rangle=\sum_{l,k''}\langle\alpha_m^{k'}|\,^{k''}lm\rangle\langle\alpha_m^k|k''lm\rangle\phi_{ll} \tag{5}$$

in terms of the field-free (and diagonal, m-independent) matrix elements of ϕ. Before describing their evaluation, we note that any additional field dependence introduced by changes in relative level positions, etc., used in the electron-scattering calculations, is almost certainly negligible because Debye-shielding effects will be seen to be more important that $\Delta n=0$ level splittings under all conditions of physical interest. For similar reasons, no significant errors are expected from the use of ϕ_{ll} values calculated for singlet levels also for triplet levels.

TABLE I. Multipliers for hydrogenic matrix elements and zero-field energies (in electron volts) of the $^k nl$ levels (see text) relative to the $n\,^1P$ levels.

n	Zero-field energy (eV)	Levels	Multipliers
2	−15.0	^1S-^1P	1.00
3	−4.4	^1S-^1P	1.00
	0.0	^1P-^1D	0.88
	−0.3	^1D-^3P	0.47
	−9.8	^3S-^3P	1.00
	−4.6	^3P-^3D	0.88
	−0.7	^3D-^1P	−0.47
4	−1.9	^1S-^1P	1.00
	0.0	^1P-^1D	0.90
	−0.1	^1D-^1F	0.97
	−0.1	^1D-^3F	0.27
	0.08	^1F-^3D	0.27
	−4.0	^3S-^3P	1.00
	−1.5	^3P-^1D	0.43
	−1.5	^3P-^3D	0.90
	−0.3	^3D-^1P	−0.43
	−0.04	^3F-^3D	0.97

III. ELECTRON BROADENING

The electron broadening of the various Stark components is controlled by the real part of ϕ, which in terms of cross sections for inelastic and elastic scattering can be written as

$$\phi_{ll}=-\tfrac{1}{2}\sum_{n',l'}\langle\sigma_{nl,n'l'},v\rangle N_e\ . \tag{6}$$

The sum is over all final states of the ion reached by electron-ion scattering, and the average over the electron velocity distribution $f(v)$ is indicated by $\langle\cdots\rangle$. We can safely neglect collisions with ground-state ions, except that the corresponding elastic scattering must be allowed for by calculating $\sigma_{nl,nl}$ using an expression in which the usual elastic scattering amplitude is replaced by the differences of these amplitudes for scattering on the nl excited state and the ground state. This modification only affects the $\Lambda=0$ (monopole) term in the multiple expansion for the interaction between free and bound electrons.

The various cross sections for $n=2$, 3, and 4 were calculated using a distorted-wave code for $\Lambda=0$, 1, 2, and 3 interactions and including enough interacting $n'l'$ levels to assure convergence of the sum in Eq. (6) to within $\sim 1\%$. (A similar accuracy is expected for the multipole expansion). The present distorted-wave approximation is formally identical to the nonunitarized Coulomb-Born

approximation, in which the elements of the reactance matrix R are expressed in terms of radial integrals involving Coulomb functions of the colliding electron. In the distorted-wave method, the Coulomb functions are replaced by functions F_{kl} describing the scattering on a potential due to the nucleus and the bound electrons (see Sec. IV), and the monopole elastic part of the R matrix elements is replaced by $\frac{1}{2}\sin 2\epsilon_l$, where ϵ_l is the phase shift. The scattering matrix therefore was not unitarized, but the error introduced into widths and shifts is always less than 1%. For example, for the strongest transition considered in our calculations, namely, $4p$-$4d$, the unitarized cross section [obtained from the relation $T=-2iR(1-iR)^{-1}$ instead of $T=-2iR$] at $E=0.2$ Ry (i.e., close to threshold) is only 1.2% smaller than the nonunitarized one, and the octupole terms contribute less than 1% to the total value. The largest absolute value of an R matrix element in this case is 0.2 (for $L^T=0$ partial contribution which represents only 1% of the total), and the values of matrix elements rapidly decrease with L^T. At higher energies, which are of real importance at temperatures considered in the paper, as well as for other types of transitions, the effect of unitarization is even smaller. The target wave functions for the ion are obtained using a semiempirical method[12] which allows for exchange. However, exchange with the free electron is neglected. This should not cause significant errors because typically very many partial waves contribute to the answer.

Again, use of the distorted-wave method as such should be practically exact, because all phase shifts, etc., are small at all relevant energies for the electron scattering on highly charged ions. For this reason, there are also no significant coupling effects between the various multipole terms.

Convergence of the partial wave series for $\Lambda=1$, $n'=n(\Delta n=0)$ transitions is very slow because of the small level separations, and because of the long-range nature of the dipole interactions. This difficulty has, however, no real significance, because correlations between free electrons cannot be ignored for these long-range interactions. Rather than attempting to solve the corresponding many-body problem, we simply cut off the sum over partial waves at

$$L=L_{\max}=\frac{mv^2}{\hbar\omega_p} , \tag{7}$$

i.e., use as screening length $\sim v/\omega_p$, where ω_p is the electron plasma frequency

$$\omega_p=(4\pi N_e e^2/m)^{1/2} . \tag{8}$$

Since the cross section depends only logarithmically on $L_{\max}$, the error corresponding to the uncertainty in $L_{\max}$ should not be more than $\sim 10\%$ for most conditions. However, it probably exceeds any errors of the scattering calculations per se.

As in our work on hydrogenic ion lines,[2] we found it convenient to compare our electron broadening calculations to the following semiclassical estimate:

$$\phi_{\rm sc}=-3\pi\left[\frac{2m}{\pi k_B T}\right]^{1/2}\left[\frac{\hbar}{m}\right]^2 N_e\left[\frac{n}{z}\right]^2(n^2-l^2-l-1) \times\left[C_{nl}+\tfrac{1}{2}\int_y^\infty e^{-x}\frac{1}{x}dx\right] , \tag{9}$$

with the parameter y determined from

$$y=\left[\frac{L_{\min}}{L_{\max}}\right]^2=\left[\frac{\hbar n^2}{2z}\right]^2\frac{\omega_p^2}{E_H k_B T} . \tag{10}$$

Here $E_H=13.6$ eV is the ionization energy of hydrogen, and $z=17$ the screened nuclear charge acting upon the nl electron (see also the discussion of the C_{nl} below). The quantity $L_{\min}$ corresponds to collisions whose impact parameters is about equal to the bound-state radius $r_n\approx n^2 a_0/z$ of the target ion. This omission of collisions with $L<L_{\min}$ is required in the semiclassical dipole approximation to avoid overestimates of the effects of close collisions. It is not needed in our distorted-wave, multipole expansion calculations, which also account for the zero-field $\Delta n=0$ level separations.

The Maxwell-averaged values of $\sum_{n',l'}\sigma_{nl,n'l'}v$, in units of $2a_0^2(\pi E_H/kT)^{1/2}e^2/\hbar$ and of a $\Delta n=0$ dipole strengh factor $6(n/z)^2(n^2-l^2-l-1)$, for $n=2$, 3, and 4 and $l=1$ are listed in Table II as functions of temperature and density. From Eqs. (6) and (9), the corresponding semiclassical expression is seen to be

$$\sum_{n',l'}\langle\sigma_{nl,n'l'}v\rangle_{\rm sc}=2a_0^2\left[\frac{\pi E_H}{k_B T}\right]^{1/2}\frac{e^2}{\hbar}6\left[\frac{n}{z}\right]^2 \times(n^2-l^2-l-1) \times\left[C_{nl}+\tfrac{1}{2}\int_y^\infty e^{-x}\frac{1}{x}dx\right] . \tag{11}$$

It was used to determine C_{nl} values by comparison with the distored-wave result, namely,

$$\sum_{n',l'}\langle\sigma_{nl,n'l'}v\rangle =2a_0^2\left[\frac{\pi E_H}{k_B T}\right]^{1/2}\frac{e^2}{\hbar}\frac{1}{2l+1} \times\sum_{n',l'}\int[\Omega(E)]_{nl,n'l'}\exp(-E/k_B T)\frac{1}{k_B T}dE , \tag{12}$$

where the $\Omega_{nl,n'l'}$ are our calculated collision strengths. Such C_{nl} values are also listed in Table II, where they are compared (at $N_e=10^{22}$ cm^{-3}) with corresponding calclations[7(a)] for hydrogen.

In Ref. 7(a), the C_{nl} values were assumed to be independent of density. We therefore make the comparison at a density where the variation of C_{nl} with density is weak. Whether or not the increase of C_{nl} with density at low temperatures is significant is questionable, because Debye shielding might then reduce other than $\Lambda=1$, $\Delta n=0$ contributions as well. The increase amounts to $\lesssim 15\%$ of the electron-produced widths. Under these conditions, errors due to uncertainties in the Debye

shielding correction of, say, ~10% in the electron broadening must therefore be expected. (Remember that errors in our distorted-wave calculations as such should be much smaller.) Differences between our C_{nl} values for He-like ions and those of Ref. 7(a) for H-like ions, except for $n=2$, correspond to smaller errors than this, and we therefore use the results of Ref. 7(a) for all nl states other than $l=1$ in our profile calculations. For $n=2$, use of C_{n1} values from Ref. 7(a) would increase collisional widths by ~10% at high densities and temperatures. We also made comparisons with recent calculations for He-like ions,[7(b)] again finding ~10% agreement.

Semiclassically, the C_{nl} may be interpreted as the contribution from strong or close collisions. In the distorted-wave calculations a corresponding term certainly arises from $\Lambda=0$ monopole interactions in the region where the radial coordinate of the scattered electron is smaller than that of the nl bound electron, and also from $\Delta n\neq 0$, $\Lambda=1$, and any $\Lambda>1$ interactions. Having nearly temperature-independent C_{nl} would have indicated a dominant role of $\Lambda=0$ collision strengths, since the variation of $\Lambda=0$ collision strenghs, summed over n', is quite small. (They decrease by less than 20% in the range from $E=E_H$ to $E=300E_H$ for the initial kinetic energy.) However, inelastic contributions from $\Lambda\geq 1$ interactions increase with energy, as various thresholds are exceeded, and are evidently quite important.

We finally mention other electron broadening processes not explicitly accounted for in the present and previous calculations. Broadening due to collisional ionization of the nl levels can be estimated according to Sampson and co-workers[13]. It usually amounts to less than 1%, except for $n=2$ at high temperatures where it reaches ~5% at $N_e=10^{24}$ cm^{-3}. Radiative recombination rates are a small fraction of a percent of the broadening rate for $n=2$ and less than that for $n>2$. Radiationless capture rates for the $1s2p$ states, mostly accompanied by excitations to $1s3d$ states with the plasma electron also going into $3d$, can be estimated to contribute about 20% of the total broadening rate at 400 eV and $N_e=10^{24}$ cm^{-3}, with the relative contribution decreasing faster than $1/T^{3/2}$. For this estimate calculated Auger rates[14] for doubly excited states of heliumlike ions were used together with the principle of detailed balancing. Capture rates for $1s3p$ and $1s4p$ are much less important in comparison to their broadening rates, both because, e.g., $3p$-$4d$ excitations are relatively less important than $2p$-$3d$ excitations, and because the threshold energies are well below k_BT in these cases.

Three-body recombination must also be considered as a line-broadening process.[15] Again using the principle of detailed balancing, we can estimate recombination rates into principal quantum number $n''=2$, 3, and 4 levels for the additional electron from the corresponding collisional ionization rates.[13] The $n''=4$ rates come to ~20% of the $n=2$ broadening rate at $k_BT=400$ eV, $N_e=10^{24}$

TABLE II. Collision strengths $\Omega_{nl,n'l'}$ for $(1snp)^1P$ levels in units of $(2l+1)6(n/z)^2(n^2-l^2-l-1)$, integrated over energy (in k_BT units) with $\exp(-E/k_BT)$ as weight factor and summed over final states. Strong collision constants C_{nl} from Eqs. (11) and (12) are in parentheses. At $N_e=10^{22}$ cm^{-3}, C_{nl} values from Ref. 7(a) are listed for comparison.

N_e (cm^{-3})		$n=2$		
k_BT (eV)	10^{22}	10^{23}	10^{24}	10^{25}
400	5.36(0.52,0.35)	4.24(0.56)	3.13(0.60)	2.30(0.90)
800	6.31(1.13,1.17)	5.17(1.14)	4.04(1.16)	3.08(1.34)
1200	6.89(1.50,1.70)	5.75(1.51)	4.61(1.52)	3.60(1.66)
1600	7.31(1.78,2.06)	6.15(1.77)	5.03(1.80)	3.98(1.90)
2000	7.62(1.97,2.32)	6.45(1.96)	5.35(2.01)	4.30(2.11)
N_e (cm^{-3})		$n=3$		
k_BT (eV)	10^{21}	10^{22}	10^{23}	10^{24}
400	5.25(0.07)	4.13(0.11,−0.05)	3.06(0.19)	2.08(0.35)
800	5.90(0.38)	4.76(0.39,0.37)	3.65(0.43)	2.59(0.52)
1200	6.26(0.53)	5.10(0.52,0.55)	3.98(0.55)	2.89(0.61)
1600	6.48(0.59)	5.33(0.61,0.66)	4.19(0.62)	3.09(0.67)
2000	6.66(0.67)	5.49(0.66,0.71)	4.36(0.68)	3.25(0.72)
N_e (cm^{-3})		$n=4$		
k_BT (eV)	10^{21}	10^{22}	10^{23}	10^{24}
400	4.90(0.30)	3.77(0.32,0.12)	2.71(0.41)	1.79(0.62)
800	5.43(0.48)	4.28(0.48,0.34)	3.17(0.52)	2.14(0.63)
1200	5.70(0.55)	4.54(0.54,0.45)	3.41(0.56)	2.34(0.63)
1600	5.88(0.58)	4.72(0.57,0.53)	3.58(0.58)	2.48(0.63)
2000	6.01(0.60)	4.84(0.58,0.59)	3.70(0.59)	2.59(0.63)

cm^{-3}, the $n''=3$ and 2 rates to $\sim 4\%$ and 0.5%, respectively, all of them decreasing rapidly with increasing temperature. Before adding these rates to the collisional linewidth, one should account for the fact that three-body recombination rates are about the same for $1s^2$ ions as for $1s2p$ ions and that, e.g., $1s^2 3d - 1s2p3d$ transition energies are often very close to the $1s^2$-$1s2p$ resonance line. Extrapolation of the results of Ref. 14 for the corresponding transitions in neon suggests that about a quarter of the recombinations into $n''=3$ and 4 levels result in satellite lines that fall within the collisional full width at half maximum (FWHM) width of the Ar XVII resonance line at $N_e = 10^{24}$ cm^{-3}, as would almost all of the $n''=5$ satellites. Therefore, the effective broadening due to three-body recombination at 400 eV, 10^{24} cm^{-3} is estimated at $\sim 15\%$. At 400 eV, 10^{25} cm^{-3} most $n''=3$ and 4 satellites are unresolved, leaving the $n''=2$ contribution and about a quarter of the $n''=3$ contribution to give again $\sim 15\%$ of the broadening rate. Effects of three-body recombination on the broadening of the lines from the $n=3$ and 4 levels are considerably smaller in relative terms, and neglecting three-body recombination is therefore not likely to cause more than 10% error in $n=3$ and 4 linewidths even at low temperatures. For $n=2$, further analysis is needed. Pending this, we propose to add 15% at low temperatures, decreasing as $1/T^2$, and to account for the radiationless capture process and for collisional ionization by also adding these rates as discussed above.

IV. SHIFTS FROM ELECTRON COLLISIONS

In almost all calculations of Stark profiles for one-electron ions, shifts were neglected. They also have eluded experimental detection,[16] at least for $z \gtrsim 6$. For ionized helium, however, there are some measurements and calculations[17] which mostly suggest relatively small red shifts from $\Lambda=1$ electron-ion collisional effects. Corresponding effects for the Ar XVII lines were estimated to be small ($\lesssim 10\%$) compared to the major collisional effect to to be discussed shortly. From the experience with He II calculations,[17] $\Lambda > 1$ contributions should be negligible as well, which leaves $\Lambda=0$ "penetrating" monopole interactions. This is not only consistent with the recent calculations for one- and two-electron ions[7] where these $\Lambda=0$ shifts were also found to be dominant, but can also be seen by estimating the otherwise dominating $\Lambda=1$, $\Delta n \neq 0$ shifts as follows: From the characteristic shift functions in semiclassical calculations [see Fig. 9(b) in Ref. 3] follows a ratio of shifts and FWHM widths $\lesssim \pi/4\Omega^*$, where the Ω^* are the reduced collision strengths in Table II. Since only interactions with levels of different principal quantum numbers ($\Delta n \neq 0$) contribute in this ratio, this estimate must still be multiplied by the relative values of $\Delta n \neq 0$ matrix elements, which can be determined from Eq. (467) of Ref. 3 to $(n^2+17)/10(n^2-1)$. These factors multiplied by $\pi/4\Omega^*$ give shift to (full) width ratios of $\lesssim 0.24$, 0.12, and 0.07, respectively. Anticipating our results for the $\Lambda=0$ shift, this suggests very strongly that $\Lambda > 0$ shifts are less than 10% of the $\Lambda=0$ shifts.

We calculated electron-collisional shifts from

$$d = -2\left[\frac{\pi E_H}{k_B T}\right]^{1/2} N_e a_0^3 \frac{e^2}{\hbar a_0} \sum_{L=0}^{\infty} (2L+1)\sin 2\Delta\epsilon_L$$
$$= -4\left[\frac{\pi E_H}{k_B T}\right]^{1/2} N_e a_0^3 \frac{e^2}{\hbar a_0} \sum_{L=0}^{\infty} (2L+1)\sin\Delta\epsilon_L \cos\Delta\epsilon_L \ , \tag{13}$$

where the $\Delta\epsilon_L$ are the differences of the $\Lambda=0$, partial-wave L phase shifts for scattering on upper and lower levels.

In the distorted-wave calculation, the phase shifts ϵ_L were determined from the asymptotic form of the radial part F_{kL} of the wave function representing the colliding electron with energy E. At large r, F_{kL} is proportional to

$$\sin[kr - \tfrac{1}{2}\pi L + \alpha \ln 2kr + \arg\Gamma(L+1-i\alpha) + \epsilon_L] \ ,$$

where $k = mv/\hbar$, $\alpha = Ze^2/\hbar v$, and Z is the asymptotic charge of the ion. F_{kL} satisfies the equation

$$\left[\frac{d^2}{dr^2} - \frac{L(L+1)}{r^2} + \frac{2m}{\hbar^2}\left[\frac{Z_n e^2}{r} - U_0 + E\right]\right] F_{kL} = 0 \ . \tag{14}$$

U_0 is the monopole part of the interaction energy of the colliding electron and two bound electrons in the $1snl$ configuration, and Z_n is the nuclear charge. The phase shifts are slowly increasing with electron energy E, and we therefore calculated the Maxwell average of the sum, using $1/v$ as weight factor. These averages for the various nl target states are presented in Table III. They agree to within $\lesssim 5\%$ with the results of Ref. 7(a), for $z=17$, where the electron-collisional shifts are written as

$$\hbar d = -\frac{10^{-22} N_e}{z^2} D \ (\text{eV}) \ . \tag{15}$$

TABLE III. Thermal averages of the sum over partial waves of the products of $\sin\Delta\epsilon_L$ and $\cos\Delta\epsilon_L$. The $\Delta\epsilon_L$ are phase shift differences for scattering on $(1snl)^1L$ and $(1s^2)^1S$ target states (see text).

$k_B T$ (eV)	2s	2p	3s	3p	3d	4s	4p	4d	4f
400	0.636	0.471	2.490	2.247	1.673	6.515	6.100	5.264	3.996
800	0.678	0.500	2.763	2.486	1.832	7.412	6.936	5.969	4.495
1200	0.717	0.527	3.010	2.700	1.969	8.103	7.596	6.540	4.916
1600	0.753	0.553	3.246	2.904	2.092	8.684	8.169	7.043	5.298
2000	0.788	0.579	3.476	3.102	2.204	9.199	8.691	7.507	5.654

The correspondence is therefore

$$D \doteq 4z^2 \left[\frac{\pi E_H}{k_B T}\right]^{1/2} 27.2\times 10^{22} a_0^3 \times \sum_{L=0}^{\infty} (2L+1)\sin\Delta\epsilon_L \cos\Delta\epsilon_L \ . \quad (16)$$

Agreement with the more recent results for He-like ions[7(b)] is equally good, confirming the above conclusions regarding $\Lambda \neq 0$ terms.

As already noted in Ref. 7(a), these shifts are relatively large, namely, comparable to the FWHM widths at high densities of the electron-broadened $n=3$ and 4 lines and over a factor of 2 larger than this width in case of $n=2$. [See Fig. 1, upper half, compared to the half width at half maximum (HWHM) widths in the lower half.] This relatively large shift is reduced some by the Stark shift of the resonance line arising from ion-produced fields or from ion-ion collisions, which is in the opposite direction. The ion impact shift and width coefficients shown in Fig. 1 for comparison with the electron effects were obtained using Eqs. (151), (185), and (195) of Ref. 3, i.e., using the impact-parameter method with characteristic width and shift functions for the repulsive case.[18] However, the impact approximation is valid even for light ions only at densities so low that Doppler broadening dominates. In Sec. V ion effects are therefore evaluated using the quasistatic approximation for the ions. This approximation is appropriate at high densities, where the shifts discussed here may be important.

At least at the highest densities for our calculations, $N=10^{25}$ cm^{-3} for $n=2$ and 3 and $N=10^{24}$ cm^{-3} for $n=4$, the electron-collisional shifts exceed thermal Doppler widths (FWHM) by factors $\sim 4-35$. For $n=3$ and 4 it is also important that the shifts of the mostly rather closely spaced nl levels are different. These differences effectively increase the overall width of these lines, but their average shifts should also be observable at high densities. Some of the electron-collisional shifts are substantially larger than predictions from (linearized) Debye or uniform electron-gas models. This is especially true for $n=2$, presumably because of the large strength of the Coulomb interaction relative to the thermal energies. We also note that the Fermi energy, e.g., $E_F=54$ eV at $N_e=10^{25}$ cm^{-3}, is well below $k_B T$ for all conditions considered here. Neglecting degeneracy of the free electrons should therefore not cause any substantial errors. However, in contrast to the width calculations, small L partial waves do dominate the calculated shifts, so that exchange with the bound electrons could be important. We therefore recalculated the shifts with exchange, finding increases of 10%, 8%, 6%, and 5% as the temperature was varied from 400 to 2000 eV. We finally point out that the phase shifts are all small so that what we calculate is actually the time average of the effective interaction. This explains the agreement with self-consistent field models[6,7] which amount to calculate the ensemble average. Also, the complications concerning the separation of static and dynamic contributions do not arise to this order.

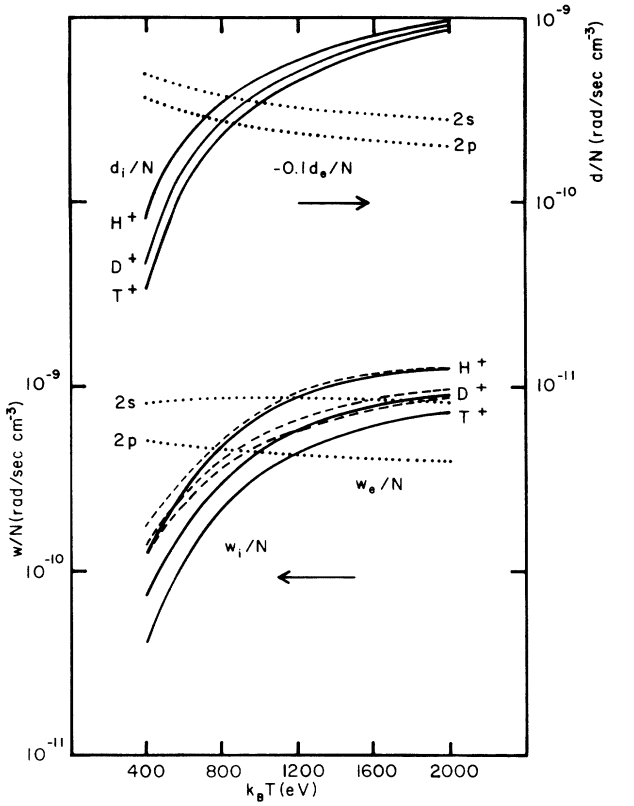

FIG. 1. Coefficients for the impact shifts (upper half) and widths (lower half) of the 1^1S-2^1P line, d/N and w/N, respectively, as functions of temperature. Shown are the corresponding contributions by the electrons (dotted curves), those for the shifts multiplied by -0.1, and those for the widths evaluated at $N_e=10^{24}$ cm^{-3}, for this line and for its forbidden component, 1^1S-2^1S. Also shown are impact-parameter method estimates for the corresponding ion collisional effects from dipole interactions (solid curves) and from dipole and quadrupole interactions (dashed curves).

V. CALCULATED LINE PROFILES AND DISCUSSION

We calculated profiles using the methods discussed in Secs. II–IV for temperatures ranging from 400 to 2000 eV and electron densities from 10^{23} to 10^{25} cm^{-3} for the resonance line ($n=2$), 10^{22} to 10^{25} cm^{-3} for $n=3$, and 10^{21} to 10^{24} cm^{-3} for the $n=4$ line. Such electron-impact, quasistatic ion profiles are shown for $k_B T=800$ eV in Figs. 2–4 as the narrowest and most structured profiles. The intermediate profiles also include thermal Doppler broadening, while the broadest and smoothest profiles were further corrected for ion-dynamical effects following Ref. 5 and assuming an equal mixture of D^+ and T^+ as perturbing ions.

The computer simulations of ion-dynamical effects in Ref. 5 were for lines of one-electron ions. We found that they could be represented to within better than 5% by convolutions of Gaussian and quasistatic profiles. The Gaussian widths, determined empirically as fit parameters and scaled according to $N_e^{5/12}T^{1/4}/M_i^{1/2}$, where M_i is the hydrogen, etc., ion mass, were then used to similarly smooth the quasistatic profiles obtained here for the

two-electron ions.

Such corrections are appropriate only for lines resembling profiles of corresponding one-electron ion lines,[2] i.e., for the $n=3$ and 4 lines and for the conditions of interest here. The $n=2$ line profiles, however, remain quite different from hydrogenic profiles even for the highest density considered. As can be seen from Figs. 2(b) and 2(c), ion-dynamical corrections are probably not important for $N_e \geq 10^{24}$ cm^{-3}, but according to Fig. 2(a) are quite important for $N_e \leq 10^{23}$ cm^{-3}. For the vicinity of the allowed line, it turns out that the ion impact width according to Fig. 1 is only 0.017 eV and the electron-impact width 0.043 eV according to Sec. III. The corresponding 0.060-eV FWHM Lorentzian width is too small to account for the broadening of the line core in Fig. 2(a) over and above the Doppler broadening. This suggests that ion-dynamical effects are actually smaller than estimated from Ref. 5. However, since Doppler broadening is dominant here, no significant errors would be incurred in applications.

The effects of additional electron broadening from three-body recombination, etc., as discussed at the end of Sec. III were found to affect pure Stark profiles by as much as 20% at the highest density and lowest tempera-

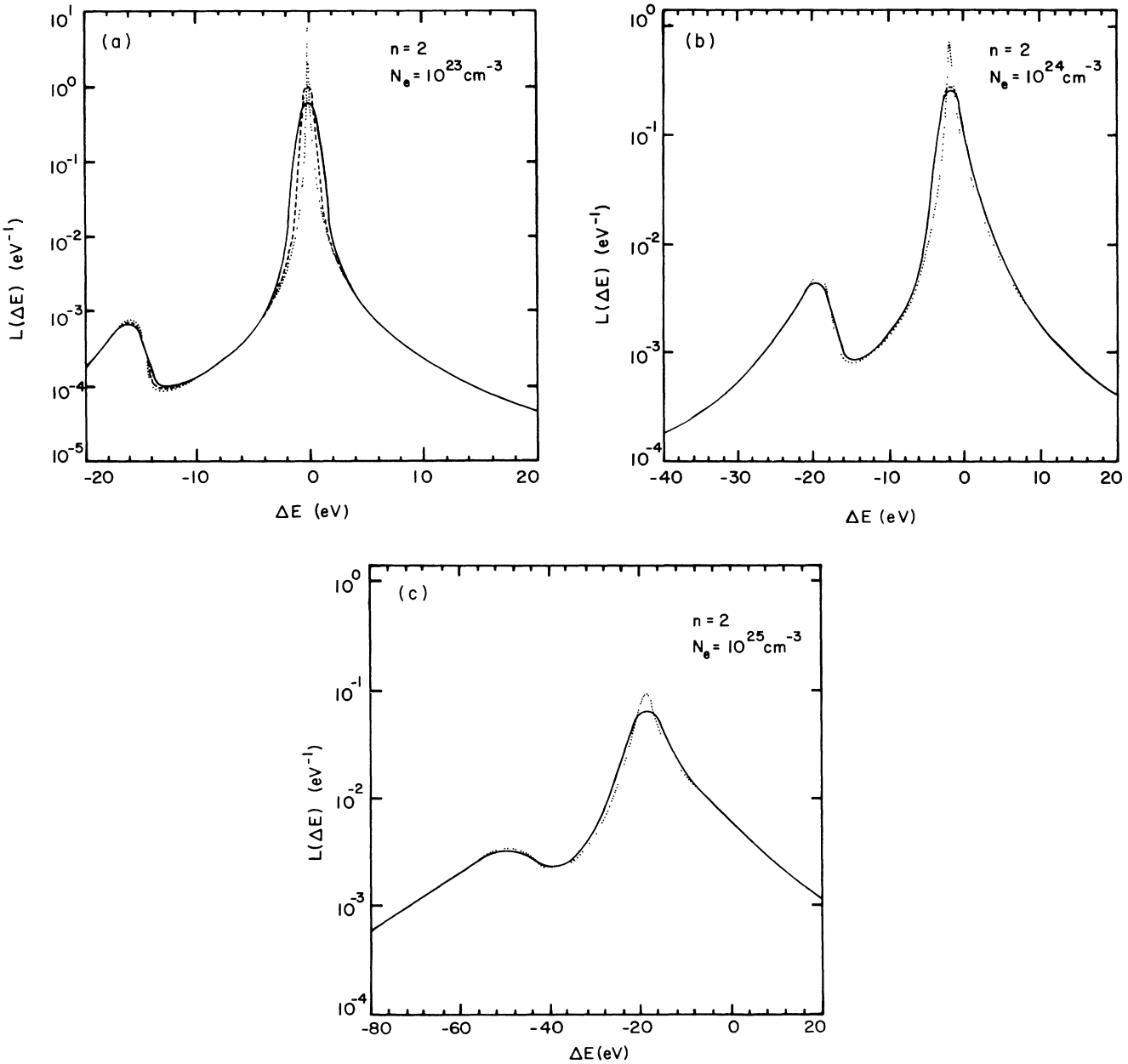

FIG. 2. Calculated profiles of the $1\,^1S$-$2\,^1P,^1S$ line at $k_BT=800$ eV and various densities. The sharpest profiles (dotted lines) include broadening by quasistatic ion fields and by electron collisions. The intermediate profiles (dashed lines) are corrected for thermal Doppler broadening, while the smoothest or broadest profiles (solid lines) have also been corrected for ion-dynamical effects (see text). The small peak at low energies corresponds to the $1\,^1S$-$2\,^1S$ forbidden Stark component.

ture. However, after allowance for quasistatic and dynamic broadening by ions and for Doppler broadening, the corresponding changes are almost always less than 5% and therefore not important.

The lines from $n=3$ and 4 shown on Figs. 3 and 4 exhibit significant Stark broadening from $N_e \approx 10^{22}$ or 10^{21} cm^{-3}, respectively. Much of the detailed structure of their pure Stark profiles at these relatively low densities is smoothed out by Doppler broadening and by the ion-dynamical corrections. However, even at $N_e \gtrsim 10^{23}$ cm^{-3}, some of the structure remains, and the lines begin to resemble rather closely calculated Ly-β and Ly-γ profiles of one-electron ions.[2] We also note that characteristic features, e.g., the separation of the two intensity maxima (see Fig. 3) and various fractional intensity widths of the $n=3$ line scale very closely as $N_e^{2/3}$ from $N_e = 10^{23}-10^{25}$ cm^{-3}.

This close adherence to the classical Holtsmark scaling in case of the $n=3$ line is not what one would expect from the ion-field distribution functions,[8] which become increasingly narrower relative to the Holtsmark distribution[3] as the density increases. Evidently this deviation from the Holtsmark scaling, which is due to Debye shielding of ions by electrons and to ion-ion correlations, is compensated by a faster than $N_e^{2/3}$ increase in the broadening caused by electrons, with a significant contribution from differences in the electron-collisional shifts of the various nl levels.

Shifts of the entire profiles are also quite noticeable, as are asymmetries. Both of these attributes are somewhat

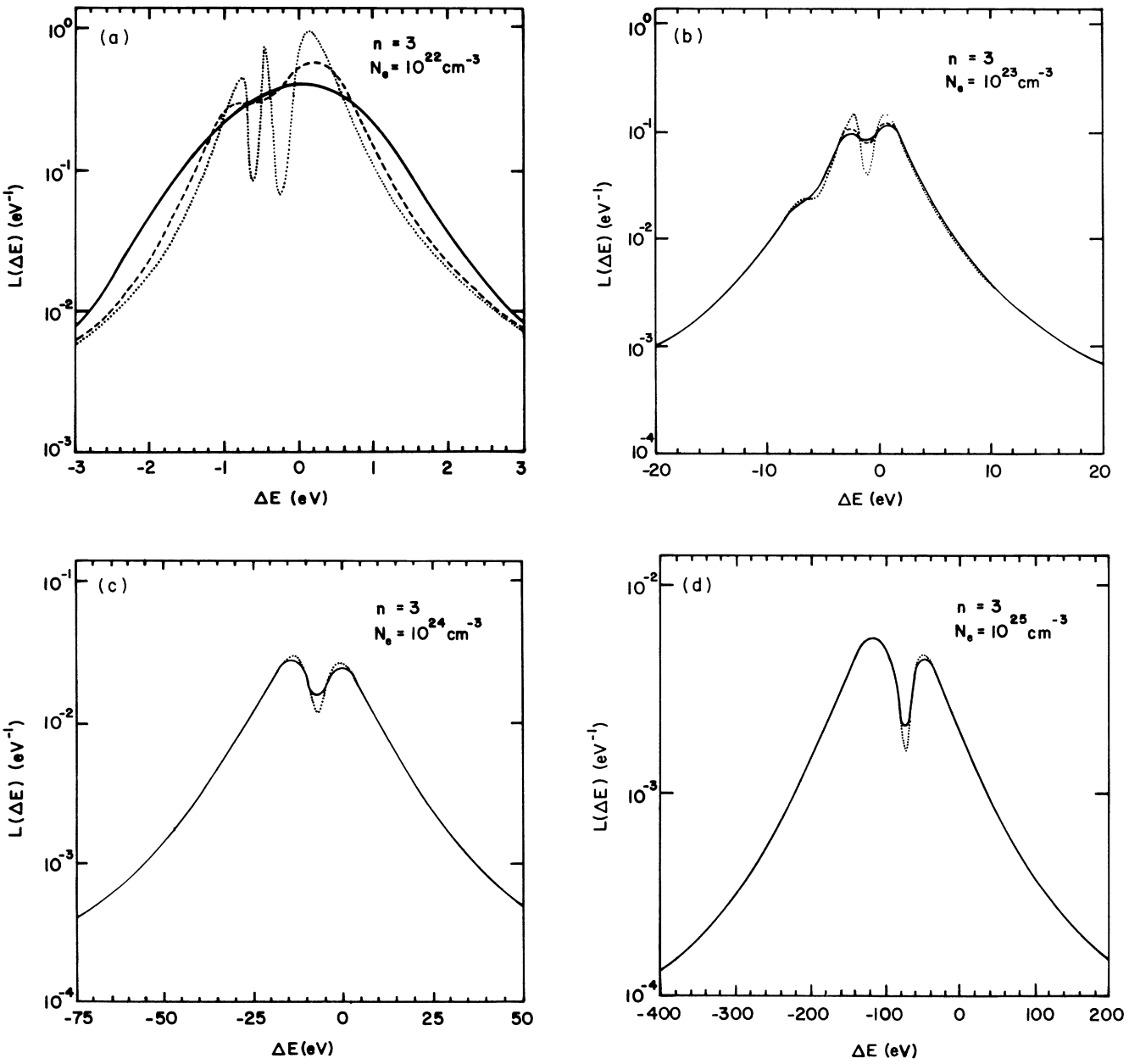

FIG. 3. Profiles as in Fig. 3 for the $1\,^1S - n=3$ singlet and triplet lines.

uncertain, because the dipole approximation was used to calculate the quasistatic broadening. However, estimates of shifts produced by quadrupole interactions, using an extrapolation with respect to the effective nuclear charge from 2 to 17 of the calculated ion-quadrupole shifts for He II lines,[17] predict shifts of only ~ 1 eV near the half-intensity points increasing to 2 or 3 eV, respectively, between $\frac{1}{4}$ and $\frac{1}{8}$ of peak intensity points, all at $N_e = 10^{25}$ cm^{-3}. Such quadrupole shifts are therefore negligible, also at lower densities, since they are linear in the density.

Profiles for $n = 4$ are shown on Fig. 4. In this case characteristic structures in the pure Stark profiles are effectively smoothed by Doppler and ion-dynamical effects at $N_e = 10^{21}$ cm^{-3}, and the profiles begin to resemble L_γ profiles as the density increases. Whether or not inclusion of higher multipole terms[19,20] in the ion-ion interaction and of interactions with $n = 5$ levels would reduce the shoulders that remain in the profiles for $N_e \gtrsim 10^{23}$ cm^{-3} is an open question, but shifts from ion-ion quadrupole interactions are again found negligibly small. Compared to the $n = 3$ line, changes in profile shapes as function of density are relatively large. Therefore we do not find a simple scaling law for half-widths, etc.

All of our calculations assume that the argon ions are not important as perturbers. At fixed electron density, the lines would probably become somewhat broader with increasing argon abundance, although reduction of ion-dynamical effects and even larger deviations from the

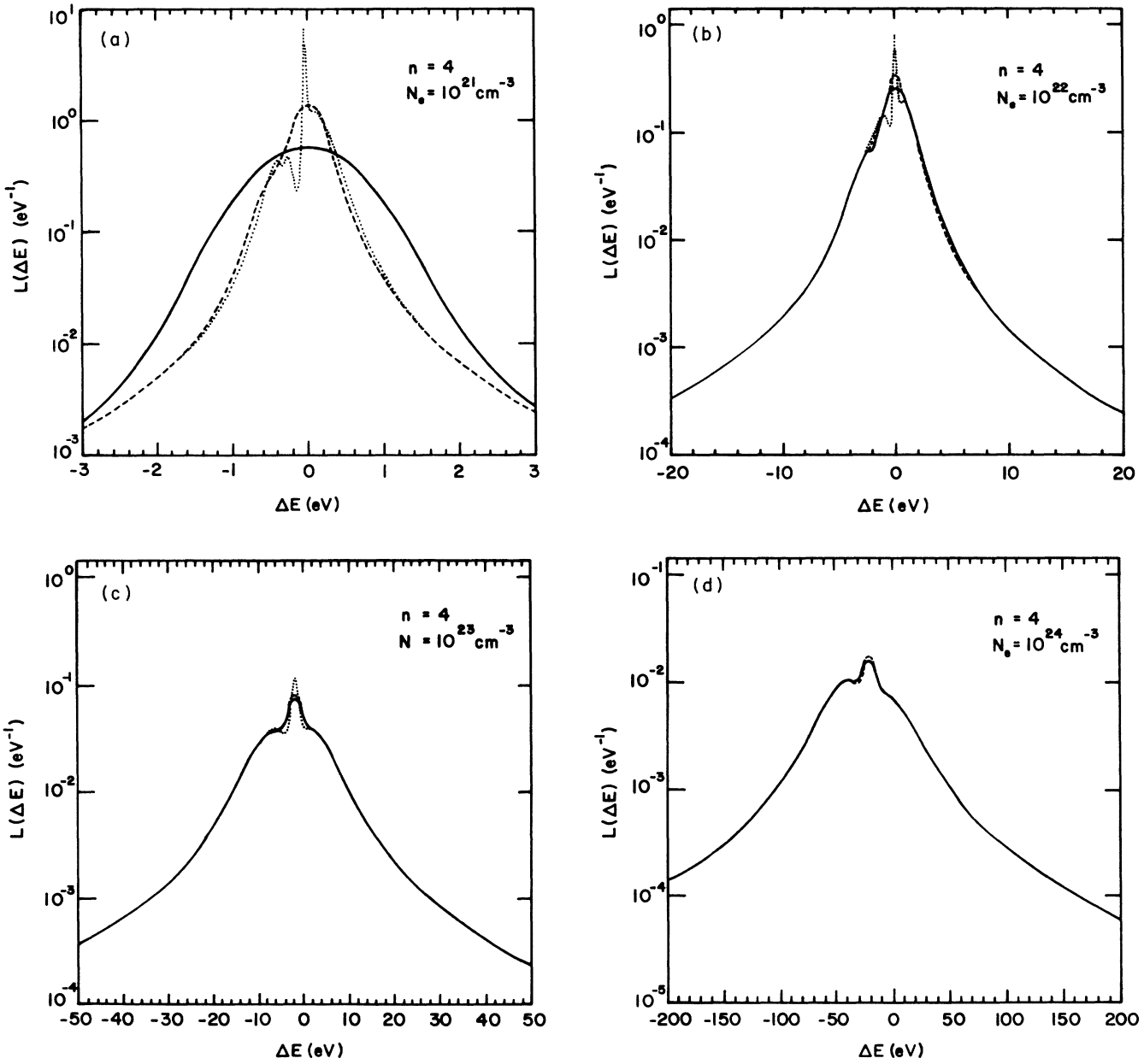

FIG. 4. Profiles as in Fig. 3 for the $1\,^1S - n = 4$ singlet and triplet lines.

Holtsmark field-strength distribution both mitigate the additional broadening. Finally, for pure argon plasmas and at the highest electron densities considered here one should probably also question the validity of the basic notion of a perturbation approach beginning with unperturbed states of isolated argon ions and free Coulomb states for the plasma electrons.

Calculations of lithiumlike and berylliumlike lines of krypton also based on the quasistatic approximation for ions but a relaxation theory dipole interaction approximation for electrons, and a comparison with laser implosion experiments were recently published be Woltz and Hooper.[21] Their method when applied to heliumlike lines should give profiles very similar to those in Figs. 2–4, except that their electron broadening and shifts would be smaller. Deviations between relaxation theory and impact approximation calculations as such would be numerically important only for the $n=3$ and 4 lines at the highest densities and for large ΔE.

Lastly, after our paper was written, recent work by Gaisinsky and Oks,[22] came to our attention which is concerned with the relative intensities of forbidden components caused by quasistatic fields. These authors estimate that quadrupole interaction shifts of the $2\,^1P$ level lead to a decrease in the relative intensity by as much as a factor of 2. However, they neglect electron effects, which are partially responsible for the $\sim$30-eV $2\,^1S-2\,^1P$ separation at $N_e=10^{25}$ cm^{-3} [see Fig. 2(c)], to be compared with a quadrupole shift of ≤ 3 eV (see above). Moreover, these authors assume that only quasistatic fields contribute to the forbidden component. This assumption is not correct, which can already be seen from the fact that oscillating fields are about as effective as dc fields in causing so-called plasma satellites.[3] We have also used a unified theory modification of the impact approximation for ions in order to estimate the line shape in the vicinity of the forbidden component, starting with Eq. (442) of Ref. 3. With an approximation for the characteristic width function corresponding to the unit Gaunt factor approximation for electrons and assuming statistical populations for the $2\,^1S$ and $2\,^1P$ populations we find integrated intensities of the forbidden component which agree within a factor of 2 with those from the quasistatic approximation at low densities. Their widths are also about the same as in Fig. 2(a), but the valley between allowed and forbidden components is shallower by about 30%. Whether or not the corresponding uncertainties in the profiles presented here would lead to observable differences between measured and calculated spectra is questionable, because Li-like satellite lines in the vicinity of the forbidden component and finite optical depth of the allowed component would have to be included in the calculations.[23]

ACKNOWLEDGMENTS

We thank Dr. David B. Boercker of the Lawrence Livermore National Laboratory for providing us with tables of ion-field-strength distribution functions and Mr. Jerry Pender for his help with the profile calculations. This research was partially sponsored by the National Science Foundation and the Office of Naval Research.

[1]Allan Hauer, K. B. Mitchell, D. B. van Hulsteyn, T. H. Tan, E. J. Linnebur, M. M. Mueller, P. C. Kepple, and H. R. Griem, Phys. Rev. Lett. **45**, 1495 (1980).

[2]H. R. Griem, M. Blaha, and P. C. Kepple, Phys Rev. A **19**, 2421 (1979).

[3]H. R. Griem, Spectral Line Broadening by Plasmas (Academic, New York, 1974).

[4]H. R. Griem and P. C. Kepple, in *Spectral Line Shapes,* edited by B. Wende (de Gruyter, Berlin, 1981), p. 391; see also R. W. Lee, G. E. Bromage and A. G. Richards, J. Phys. B **12**, 3445 (1979).

[5]R. Stamm, B. Talin, E. L. Pollock, and C. A. Iglesias, Phys. Rev. A **34**, 4144 (1986).

[6]J. Davis and M. Blaha, J. Quant. Spectrosc. Radiat. Transfer **27**, 307 (1982).

[7]H. Nguyen, M. Koenig, D. Benredjem, M. Caby, and G. Coulaud, Phys. Rev. A **33**, 1279 (1986); M. Koenig, P. Malnoult, and H. Nguyen, *ibid.* **38**, 2089 (1988).

[8]R. J. Tighe and C. F. Hooper, Jr., Phys. Rev. A **15**, 1773 (1977); C. A. Iglesias, J. L. Lebovitz, and D. MacGowan, *ibid.* **28**, 1667 (1983); and J. W. Dufty, D. B. Boercker, and C. A. Iglesias, *ibid.* **31**, 1681 (1985).

[9]R. D. Cowan (private communication).

[10]W. C. Martin, Phys. Scr. **24**, 725 (1981).

[11]G. W. F. Drake, Phys. Rev. A **19**, 1387 (1979).

[12]M. Blaha and J. Davis, J. Quant. Spectrosc. Radiat. Transfer **19**, 227 (1978).

[13]L. B. Golden and D. H. Sampson, J. Phys. B **10**, 2229 (1977); D. L. Moores, L. B. Golden, and D. H. Sampson, *ibid.* **13**, 385 (1980); and R. E. H. Clark, and D. H. Sampson, *ibid.* **17**, 3311 (1984).

[14]K. R. Karim, C. P. Bhalla, and T. W. Tunnel, J. Quant. Spectrosc. Radiat. Transfer **36**, 505 (1986).

[15]J. C. Weisheit, in Proceedings of the Xth International Conference on Atomic Physics, II, 117, Tokyo, 1986, edited by H. Narumi and I. Shimamura (North-Holland, Amsterdam, 1987), p. 544.

[16]S. Goldsmith, H. R. Griem, and L. Cohen, Phys. Rev. A **30**, 2775 (1984).

[17]H. R. Griem, Phys. Rev. A **27**, 2566 (1983); see also Phys. Rev. A **38**, 2943 (1988).

[18]S. Sahal-Brechot, Astron. Astrophys. **1**, 91 (1969).

[19]D. Lambert and M. Louis-Jacquet, J. Phys. (Paris) **46**, 379 (1985).

[20]R. F. Joyce, L. A. Woltz, and C. F. Hooper, Jr., Phys. Rev. A **35**, 2228 (1987).

[21]L. A. Woltz and C. F. Hooper, Jr., Phys. Rev. A **38**, 4766 (1988).

[22]I. M. Gaisinsky and E. A. Oks, J. Quant. Spectrosc. Radiat. Transfer **41**, 235 (1989).

[23]C. F. Hooper, Jr., D. Kilcrease, L. Woltz, R. C. Mancini, D. K. Bradley, P. A. Jaanimagi, and M. C. Richardson, Phys. Rev. Lett. **63**, 267 (1989).